

## Model for infrared and Raman studies of molecular rotations in liquids and gases

S DATTAGUPTA and A K SOOD

Reactor Research Centre, Kalpakkam 603 102

MS received 30 April 1979; revised 18 August 1979

**Abstract.** Experimental infrared and Raman data for molecular rotations in dense phases often lie in between the results predicted by the *J*- and *M*-diffusion models of Gordon. In this paper, we present a theory which is similar in its basic approach to Gordon's extended diffusion models (EDM) but in which the restrictions of the *J* and *M* limits are removed. The outcome is a scheme which allows one to describe situations which fall between the two extreme pictures of the *J* and *M* models. Application of this scheme to experiments is discussed.

**Keywords.** Molecular rotations; infrared line shapes; Raman line shapes; generalised extended diffusion models.

### 1. Introduction

Molecular rotations in dense phases as studied by Raman and infrared spectroscopy is an important subject of activity. It has been widely reviewed in numerous articles and monographs (e.g. Gordon 1968; Steele 1976; Berne and Pecora 1976; McClung 1977, etc.). For an isotropic system such as a gas or a liquid, the investigation of vibration-rotation bands involving transitions between molecular vibrational levels reveals quantitative information about the nature of rotational motion and through it, important knowledge of inter-molecular torques. In many cases, one is concerned with linear, symmetric top or spherical molecules which have at least one axis of symmetry. Furthermore, the coupling between vibrational, translational and rotational motions is such that the respective contributions can be separated. In such a situation (the subject of the present paper), the rotational contribution to both the infrared and depolarised Raman line shapes is contained in the following correlation function (Gordon 1968):

$$C_l(t) = \langle P_l(\cos \theta(t)) \rangle, \quad (1)$$

where vibrations parallel to the symmetry axis are considered. In (1),  $l$ , the order of the Legendre polynomial  $P_l$ , is equal to one and two respectively in the infrared and Raman cases. The angle  $\theta(t)$  measures the deviation of the symmetry axis of the molecule in time  $t$ . The time-variation of  $\theta(t)$  occurs due to the coupling of the 'molecule of interest' with all the other molecules of an interacting many-body system, and the angular bracket  $\langle \dots \rangle$  denotes an average over the statistical properties of such a system.

A major breakthrough in the understanding of rotational line shapes of molecules has been the introduction by Gordon (1966) of his extended diffusion models (EDM). In these, the molecule is assumed to undergo free rotations unless interrupted by random instantaneous collisions which may alter its state of motion. Two versions of the EDM were worked out by Gordon (1966) in analytic forms for the case of a linear molecule—the *J*- and *M*-diffusion models. A feature that is common to both these is that a collision completely randomises the direction of the angular velocity. In addition, in the *J*-diffusion model, even the magnitude of the angular velocity is assumed to be randomised by a collision to its thermal equilibrium value, while it is assumed to stay constant in the *M*-diffusion case. The EDM were later applied to spherical (McClung 1969, 1971a, b; Mountain 1971) and symmetric-top (St. Pierre and Steele 1972; McClung 1972) molecules. Since the EDM properly take into consideration the inertia effects of free rotation, they yield the correct short-time behaviour of  $C_l(t)$ . Also, in the limit in which the collisions are very rapid, the result of the *J*-diffusion model agrees with that of the rotational diffusion model (Favro 1960), the expected feature. The EDM are therefore able to provide a unified picture of rotational motions from the gas-like phase in which free motions dominate to the dense liquid situation in which collisional effects take over. It may be mentioned that even if the density of a liquid is high, the free (more accurately, 'torque-free') motion can still be important if the anisotropy of the interaction is small.

Due to their inherent conceptual simplicity and yet a wide applicability over a large time-domain, the EDM of Gordon remain, to this date, the most extensively used models for the analysis of infrared and Raman rotational line shapes (McClung 1977). However, a detailed comparison of the EDM results with experimental data on a variety of systems reveals that in good many cases, the data lie somewhere in between the pictures painted by the *J*- and *M*-models (McClung 1977; Marsault *et al* 1975). The situation is roughly like this. For short times, both the *J*- and *M*-models agree with one another, and give a satisfactory account of the data points for  $C_l(t)$ . For a gas-like system, the *M*-diffusion results seem to agree with data even at long times. The *J*-diffusion model, on the other hand, explains better the long-time behaviour of  $C_l(t)$  for liquids in which collisional effects dominate (Marsault *et al* 1975). It should therefore be desirable to generalise the EDM in order to obtain a satisfactory agreement with the data for  $C_l(t)$  of a liquid as it exhibits progressively a gas-type to a diffusive behaviour with increasing density.

In § 2 we present the model and its mathematical solution. For the purpose of keeping the mathematical discussion lucid, we restrict ourselves to the case of linear molecules throughout the paper. The basic idea in setting up the model is akin to that of Gordon and like him, we also assume that the molecules, in between free rotations, are subject to abrupt collisions whose roles are to completely randomise the direction of the angular velocity. However, unlike in the treatment of Gordon, the effect of a collision in so far as causing a change in the angular speed is concerned, is taken into account in a much more general way in terms of a collision operator. Specific forms of this collision operator can then be assumed to describe different physical situations. This is illustrated in § 3 by deriving as limiting cases the results of the *M*- and the *J*-diffusion models. We then consider a certain structure of the collision operator which yields a closed-form solution of the correlation function that interpolates smoothly between the *M*- and *J*-diffusion limits. In § 4, the interpolation model is applied in deriving infrared and Raman line shapes and correlation

times. The usefulness of the interpolation model in explaining experimental data on molecular rotations, which cannot be satisfactorily accounted for by the EDM, is demonstrated in § 5. § 6 is a summary together with some comments on the limitations of the present study and possible avenues for refinement.

## 2. Mathematical formulation

### 2.1. Notations

The basic theoretical problem is to calculate the correlation function in (1) which, from the spherical harmonics addition theorem (Edmonds 1957), can be rewritten as

$$C_l(t) = 4\pi (2l+1)^{-1} \sum_{m=-l}^{+l} \langle Y_{lm}^* (\theta(0), \phi(0)) Y_{lm} (\theta(t), \phi(t)) \rangle, \quad (2)$$

where the arguments of the spherical harmonics  $Y_{lm}$  are the Euler angles defining the orientations of the molecular symmetry axis at times 0 and  $t$ .

For the sake of brevity, we shall henceforth drop the subscript  $l$ . Also, for a fixed  $l$ , we may regard  $Y_{lm}(\theta, \phi)$  ( $m = -l, \dots, l$ ) as the components of a vector  $\mathbf{Y}$  in a  $(2l+1)$  dimensional linear vector space. Equation (2) can then be expressed symbolically in the form of a dot product:

$$C_l(t) = 4\pi(2l+1)^{-1} \langle \mathbf{Y}(\theta(0), \phi(0)) \cdot \mathbf{Y}(\theta(t), \phi(t)) \rangle. \quad (3)$$

At this stage we introduce a time-development operator  $\mathcal{U}(t)$  defined by

$$\mathbf{Y}(\theta(t), \phi(t)) = \mathcal{U}(t) \mathbf{Y}(\theta(0), \phi(0)). \quad (4)$$

The operator  $\mathcal{U}(t)$  is clearly a  $(2l+1) \times (2l+1)$  dimensional matrix.

If the random process which governs the change in the molecular orientation is assumed to be stationary, the correlation function  $C_l(t)$  should be independent of the choice of the initial conditions. Therefore, for simplicity, we may set

$$\theta(0) = \phi(0) = 0. \quad (5)$$

In that case, the correlation function, using (2) to (5), can be put into the compact form

$$C_l(t) = \langle \mathcal{U}_{00}(t) \rangle, \quad (6)$$

where the subscript zero refers to the  $m = 0$  component.

To illustrate the meaning of  $\mathcal{U}(t)$ , let us consider the *free* rotation of a linear molecule which can be assumed to occur in the  $XZ$  plane. In that case,  $\mathcal{U}(t)$  is simply a rotation operator (for angular momentum  $l$ ) describing a rotation about the space-fixed  $Y$ -axis with an angular speed  $\omega$ . Thus

$$\mathcal{U}(t) = \mathcal{D}^{(l)}(0, \omega t, 0), \quad (7)$$

and for the  $l = 1$  case

$$C_1(t) = \langle \mathcal{D}_{00}^{(1)}(0, \omega t, 0) \rangle = \langle d_{00}^1(\omega t) \rangle = \langle \cos \omega t \rangle, \quad (8)$$

the expected answer. The angular bracket in (8), in the free rotor case, specifies simply an average over the thermal distribution of  $\omega$ . Here, and throughout the rest of this paper, we follow Edmonds (1957) in our notations of rotation operators.

As mentioned in § 1, we treat here the linear rotor case. At time zero, the molecule, aligned with the space-fixed  $Z$ -axis, starts rotating in a plane normal to the  $XY$ -plane (figure 1). The angular velocity of the rotor is therefore, a two-dimensional vector which lies in the  $XY$ -plane. Using plane polar co-ordinates, the direction of the angular velocity vector, and therefore, the orientation of the plane of rotation, is completely specified by the angle  $\phi$  measured from the space-fixed  $X$ -axis (figure 1). Typically, a free rotation for a time  $t$  with an angular velocity  $\omega$  can be described by the rotation operator

$$\mathbf{R}(t) = \exp [-i(\vec{\omega} \cdot \vec{L})t] = \exp [-it(\omega_X L_X + \omega_Y L_Y)], \quad (9)$$

where  $L_X$  and  $L_Y$  are the generators of rotation in the  $(2l+1)$ -dimensional vector space in which the spherical harmonics form the basis functions.\*

## 2.2. Effect of collisions

The time-interval 0 to  $t$  is divided into  $(n+1)$  parts at  $t_1, t_2, \dots, t_n$  at which points in time, the molecule is assumed to suffer instantaneous collisions (the impact approximation). In between collisions, the molecule is supposed to behave like a free rotor.

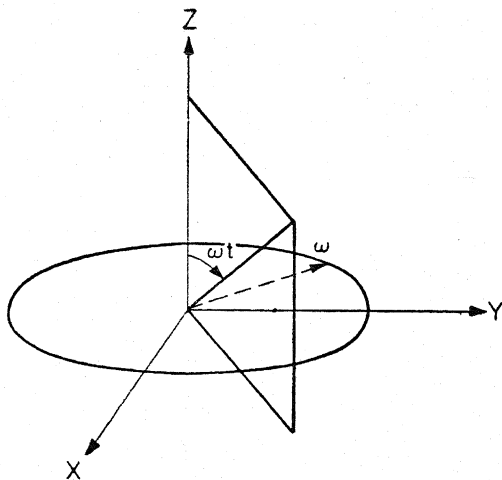


Figure 1. Geometry of rotation of a linear molecule.

\*Note that  $L$  is *not* the quantum angular momentum operator of the linear rotor and that the latter is, after all, treated classically.

The effect of a collision is assumed to be two-fold: (i) an abrupt change in the plane of rotation, i.e. the angle  $\phi$  caused by a rotation about the space-fixed  $Z$ -axis, and (ii) a change in the angular speed. The time-development operator  $\mathcal{U}(t)$  may therefore be constructed as\*\*

$$\mathcal{U}(t) = \mathcal{R}_n(t-t_n) \dots \mathcal{T}_2 \mathcal{R}_2(t_2-t_1) \mathcal{T}_1 \mathcal{R}_1(t_1), \quad (10)$$

where, for example,

$$\mathcal{R}_n(t-t_n) = \exp[-i(\vec{\omega}_n \cdot \vec{L})(t-t_n)], \quad (11)$$

$$\text{and} \quad \mathcal{T}_n = \exp(i\phi_n L_z), \quad (12)$$

$\omega_n$  being the angular velocity in the  $(n+1)$ th step, and  $\phi_n$  the *change* in the azimuthal angle resulting from the  $n$ th collision.

As in the EDM of Gordon (1966), we assume that the changes in  $\phi$  due to collisions are uncorrelated to each other and are completely arbitrary. This means that the average of  $\mathcal{U}(t)$  over a distribution of the  $\phi$ 's denoted by  $\mathcal{U}_\phi$ , factors into a product of uncorrelated averages:

$$(\mathcal{U}(t))_\phi = \mathcal{R}_n(t-t_n) \dots (\mathcal{T}_2)_\phi \mathcal{R}_2(t_2-t_1) (\mathcal{T}_1)_\phi \mathcal{R}_1(t_1). \quad (13)$$

In the above,

$$(\mathcal{T}_1)_\phi = (\mathcal{T}_2)_\phi = \dots (\mathcal{T}_n)_\phi = \frac{1}{2\pi} \int_0^{2\pi} d\phi \exp(i\phi L_z). \quad (14)$$

Note that

$$\langle m | (\mathcal{T}_1)_\phi | m' \rangle = \delta_{mm'} \delta_{m0}. \quad (15)$$

The relevant matrix element of  $(\mathcal{U}(t))_\phi$  that contributes to the correlation function (cf., equation (6)) is given from (13) and (15) by

$$\begin{aligned} \langle 0 | (\mathcal{U}(t))_\phi | 0 \rangle &= \langle 0 | \mathcal{R}_n(t-t_n) | 0 \rangle \dots \langle 0 | \mathcal{R}_2(t_2-t_1) | 0 \rangle \\ &\times \langle 0 | \mathcal{R}_1(t_1) | 0 \rangle. \end{aligned} \quad (16)$$

Since *any* direction in the  $XY$ -plane can be brought to the  $Y$ -axis *via* a rotation about  $Z$ , it is convenient to write

$$\langle 0 | \mathcal{R}_n(t) | 0 \rangle = \langle 0 | \exp(-i\omega_n L_y t) | 0 \rangle, \quad (17)$$

\*\*The instants  $t_1, t_2, \dots, t_n$  and the number  $n$  of collisions are of course summed over in the final expression for the correlation function (see (29)).

where the last step follows from the fact that the matrix elements in (17) are taken between eigenstates of  $L_z$  with eigenvalue *zero*. Denoting

$$d_n(t) = \exp(-i\omega_n L_y t), \quad (18)$$

we can rewrite (16) as

$$\begin{aligned} \langle 0 | (\mathcal{U}(t))_\phi | 0 \rangle &= \langle 0 | d_n(t-t_n) | 0 \rangle \dots \\ &\times \langle 0 | d_2(t_2-t_1) | 0 \rangle \langle 0 | d_1(t_1) | 0 \rangle. \end{aligned} \quad (19)$$

Let  $\langle 0 | (\mathcal{U}(t))_\phi | 0 \rangle \equiv G(t)$ ,

$$\langle 0 | d_n(t-t_n) | 0 \rangle \equiv g_n(t-t_n); \quad (20)$$

we then have

$$G(t) = g_n(t-t_n) \dots g_2(t_2-t_1) g_1(t_1). \quad (21)$$

### 2.3. Solution

The mathematical approach we have adopted is closest in spirit to that of Fixman and Rider (1969). Albeit the formulation given here is different from the one used by Gordon (1966), the results upto this point are completely equivalent to those of Gordon. Unlike Gordon, however, we *do not* rightaway specialise to the *J*- or *M*-diffusion models by making specific assumptions about the  $\omega$ 's in the various diffusion steps (see § 1). Instead, we regard  $\omega$  as a random variable, and introduce a matrix  $\Omega$  which is diagonal and whose elements are the possible values of the angular speed:  $\omega_1, \omega_2, \dots, \omega_n$ . We also introduce a collision operator  $\mathcal{T}$  whose element  $(\omega | \mathcal{T} | \omega')$ , for example, defines the probability of transition of the angular speed from  $\omega'$  to  $\omega$  due to a collision. In the linear vector space spanned by the  $\omega$ -variables,  $G$  and  $g$ , themselves, are matrices, and we may write from (21),

$$\tilde{G}(t) = \tilde{g}(t-t_n) \dots \mathcal{T} \tilde{g}(t_2-t_1) \mathcal{T} \tilde{g}(t_1), \quad (22)$$

where  $\tilde{g}(t) = \langle 0 | \exp(-i\Omega L_y t) | 0 \rangle$  (cf., (18) and (20)), (23)

and  $\Omega$  is defined to be such that

$$(\omega | \Omega | \omega') = \omega \delta(\omega - \omega'). \quad (24)$$

The meaning of (22) becomes clear when we examine a specific matrix element of  $\tilde{G}(t)$ . Using (23) and (24), we may write from (22),

$$\begin{aligned} (\omega | \tilde{G}(t) | \omega_0) &= \int \langle 0 | \exp(-i\omega L_y(t-t_n)) | 0 \rangle \dots (\omega_2 | \mathcal{T} | \omega_1) \\ &\times \langle 0 | \exp(-i\omega_1 L_y(t_2-t_1)) | 0 \rangle (\omega_1 | \mathcal{T} | \omega_0) \\ &\times \langle 0 | \exp(-i\omega_0 L_y t_1) | 0 \rangle d\omega_1 d\omega_2 \dots \end{aligned} \quad (25)$$

Equation (25) describes a particular collision chain with angular speeds  $\omega_0$  at  $t=0$  and  $\omega$  at  $t$ . At  $t_1$ , a collision occurs which has a probability  $(\omega_1 | \mathcal{T} | \omega_0)$  of changing instantaneously the angular speed from  $\omega_0$  to  $\omega_1$ . The molecule then rotates freely with the new speed  $\omega_1$  until  $t_2$  at which point another collision changes the angular speed, and so on. Clearly, we have to consider all possible intermediate angular speeds so that we integrate over  $\omega_1, \omega_2$ , etc. In addition we have to take into account collision chains with all possible end points so that the quantity which enters into the calculation of the correlation function is given by

$$(\tilde{G}(t))_{\text{av}} = \int d\omega_0 d\omega p(\omega_0) (\omega | \tilde{G}(t) | \omega_0), \quad (26)$$

where  $p(\omega)$  is the thermal equilibrium probability distribution of  $\omega$ . Assuming the latter to be a Maxwellian, we have for a linear molecule,

$$p(\omega) d\omega = (I/k_B T) \exp(-I\omega^2/2k_B T) \omega d\omega, \quad (27)$$

where  $I$  is the moment of inertia of the molecule,  $T$  the temperature and  $k_B$  the Boltzmann constant.

The model presented above, in which one views a random process as consisting of a chain of collision events with a transition operator associated with each collision, has been employed also in other line shape problems such as relaxation effects in Mössbauer spectra (Clauser and Blume 1971, Dattagupta 1975, 1977a) and collision broadening of spectral lines in gases (Dattagupta 1977b). Although the form of the transition matrix  $\mathcal{T}$  may vary in different contexts, both in terms of physical contents as well as mathematical complexity, the basic strategy for obtaining the correlation function is the same. This involves an averaging over the location in time of the collisions with an assumed Poissonian distribution and determining the Laplace transform of  $C_I(t)$ . Defining the latter by

$$C_I(p) \equiv \int_0^\infty C_I(t) \exp(-pt) dt, \quad (28)$$

we may write, from (6), (20), (22) and (26),

$$C_I(p) = \int d\omega_0 d\omega p(\omega_0) (\omega | [(g(p+\lambda))^{-1} - \lambda \mathcal{T}]^{-1} | \omega_0), \quad (29)$$

where  $\lambda$  is the average rate of collisions and  $g(p+\lambda)$ , from (23), is given by

$$g(p+\lambda) = \langle 0 | (p+\lambda + i\Omega Ly)^{-1} | 0 \rangle. \quad (30)$$

In deriving (29), we have omitted details for which we refer the reader to the papers mentioned in this paragraph.

### 3. Models for $\mathcal{T}$

Equation (29) constitutes a generalisation of the EDM results of Gordon in the sense that the theory now has a greater flexibility in its ability to consider various forms of

the transition operator  $\mathcal{T}$ . We discuss this below by first deriving some old results and then obtaining additional new expressions.

### 3.1. The $M$ -diffusion model

In this, it is assumed that the angular speeds do not change due to collisions, i.e.,

$$(\omega | \mathcal{T} | \omega_0) = \delta(\omega - \omega_0). \quad (31)$$

In view of (24), (29) then yields

$$C_I^M(p) = \int d\omega p(\omega) [(f(p + \lambda))^{-1} - \lambda]^{-1}, \quad (32)$$

where, from (30)

$$\begin{aligned} f(p + \lambda) &= \langle 0 | [p + \lambda + i\omega L_y]^{-1} | 0 \rangle \\ &= \int_0^\infty \exp(-(p + \lambda)t) d_{00}^{(t)}(\omega t) dt, \end{aligned} \quad (33)$$

having made use of the definitions (28) and (18).

Equation (32) is the usual  $M$ -diffusion model result (cf., equation (2.49) of Steele 1976).

### 3.2. The $J$ -diffusion model

In this case, it is assumed that every collision completely randomises the angular speed to its thermal equilibrium value. This means that the matrix element  $(\omega | \mathcal{T} | \omega_0)$  is independent of the initial angular speed  $\omega_0$ , and depends on  $\omega$  through the distribution function  $p(\omega)$ :

$$(\omega | \mathcal{T} | \omega_0) = p(\omega), \quad (34)$$

where  $p(\omega)$  is given by (27). Note that the choice of (34) is consistent with the probability conservation condition:

$$\int (\omega | \mathcal{T} | \omega_0) d\omega = 1, \quad (35)$$

and the detailed balance relation:

$$p(\omega_0) (\omega | \mathcal{T} | \omega_0) = p(\omega) (\omega_0 | \mathcal{T} | \omega). \quad (36)$$

Equations (35) and (36) are also, of course, satisfied in the  $M$ -diffusion model.

Using a matrix identity:

$$A^{-1} = B^{-1} + B^{-1}(B - A)A^{-1}, \quad (37)$$



We can write, from (29),

$$C_i^J(p) = \int d\omega_0 \, d\omega \, p(\omega_0) (\omega | g(p+\lambda) | \omega_0) \\ + \lambda \int d\omega_0 \, d\omega \, p(\omega_0) (\omega | g(p+\lambda) \mathcal{T} [(g(p+\lambda))^{-1} - \lambda \mathcal{T}]^{-1} | \omega_0). \quad (38)$$

Applying the closure property:

$$\int d\omega' | \omega' \rangle \langle \omega' | = 1, \quad (39)$$

twice to the second term on the right of (38), and making use of (34), we can show

$$C_i^J(p) = [(C_i^0(p+\lambda))^{-1} - \lambda]^{-1}, \quad (40)$$

where 
$$C_i^0(p+\lambda) = \int d\omega_0 \, d\omega \, p(\omega_0) (\omega | g(p+\lambda) | \omega_0)$$

$$= \int d\omega \, p(\omega) f(p+\lambda), \quad (41)$$

from (33), (30) and (24). Equation (40) can be shown to be identical to the result quoted for the  $J$ -diffusion model (cf., equation (2.48) of Steele (1976)).

### 3.3. Interpolation model

As is evident from the above discussion, the  $J$ - and  $M$ -diffusion models describe two extreme pictures and physical situations are expected to lie somewhere in between. In order to tackle such a case, we present below a very simple and yet a physically interesting form of  $\mathcal{T}$  which interpolates smoothly between the  $J$ - and  $M$ -limits. We assume

$$(\omega | \mathcal{T} | \omega_0) = \gamma p(\omega) + (1-\gamma) \delta(\omega - \omega_0), \quad 0 \leq \gamma \leq 1. \quad (42)$$

Therefore, if  $\gamma=0$ , we have the  $M$ -diffusion case (cf., equation (31)) while  $\gamma=1$  corresponds to the  $J$ -diffusion case (cf., equation (34)). Also,  $\gamma=0.2$ , for example, implies that a collision has an 80% probability of keeping the angular speed constant and 20% probability of randomising it to the thermal equilibrium value. Note that (42) too is consistent with (35) and (36). An identical form of the collision operator as in (42) has been considered earlier by Fixman and Rider (1969) in the case of spherical molecules.

To apply (42) to (29), we write  $\mathcal{T}$  as

$$\mathcal{T} = \gamma \mathcal{T}_1 + (1-\gamma) \mathbf{1}, \quad (43)$$

where  $\mathcal{T}_1$  is defined by

$$(\omega | \mathcal{T}_1 | \omega_0) = p(\omega) \text{ (cf., equation (42))}. \quad (44)$$

Using (37) as before, (29) can be expressed as

$$C_I^I(p) = \int d\omega_0 d\omega(\omega | g_1(p+\lambda) | \omega_0) \\ + (\gamma\lambda) \int d\omega_0 d\omega p(\omega_0) (\omega | g_1(p+\lambda) \mathfrak{I}_1 [(g(p+\lambda))^{-1} - \lambda \mathfrak{I}]^{-1} | \omega_0), \quad (45)$$

where  $g_1(p+\lambda) = [(g(p+\lambda))^{-1} - \lambda(1-\gamma)]^{-1}$ . (46)

Making use of the same mathematical steps as in (39) to (41), we now derive

$$C_I^I(p) = [(\int d\omega p(\omega) f_1(p+\lambda))^{-1} - \gamma\lambda]^{-1}, \quad (47)$$

where  $f_1(p+\lambda) = [(f(p+\lambda))^{-1} - \lambda(1-\gamma)]^{-1}$ , (48)

$f(p+\lambda)$  being given by (33). It is easy to check that in the limits  $\gamma=0$  and  $\gamma=1$ , (47) reduces to the  $M$ - and  $J$ -diffusion results of (32) and (40) respectively. It should be stressed that (47) *does not* simply constitute an interpolation between the correlation functions themselves. Thus  $C_I^I(p)$  in (47) is *not* just equal to

$$\gamma C_I^J(p) + (1-\gamma)C_I^M(p),$$

and is much richer in structure. A physical meaning of the parameter  $\gamma$  is given in Appendix A.

#### 4. Applications of the interpolation model

##### 4.1. The infrared case

As mentioned in § 1, the infrared case corresponds to  $l=1$ . Equation (33) then reduces to

$$f(p+\lambda) = \left[ (p+\lambda) + \frac{\omega^2}{(p+\lambda)} \right]^{-1}. \quad (49)$$

From (48),

$$f_1(p+\lambda) = \left[ (p+\gamma\lambda) + \frac{\omega^2}{(p+\lambda)} \right]^{-1}, \quad (50)$$

The infrared line shape, defined by  $\pi^{-1}$  times the real part of  $C_I^I(p)$ , can now be obtained from (47) and (50) for the interpolation model (see also the appendix B). Figure 2a shows the line shape for  $\lambda=0.3$  for three different values of  $\gamma$ :  $\gamma=0$  ( $M$ -diffusion),  $\gamma=1$  ( $J$ -diffusion) and  $\gamma=0.5$  (an intermediate case).<sup>\*</sup> The line profile for  $\lambda=2.5$  for the same values of  $\gamma$  are shown in figure 2b. The two values of  $\lambda$  are chosen to correspond to gas like behaviour (figure 2a) and highly hindered rotation (figure

<sup>\*</sup>The frequency and time in all our plots are expressed in reduced units of  $(k_B T/I)^{\frac{1}{2}}$  and  $(I/K_B T)^{\frac{1}{2}}$  respectively.

2b). In figures 3a and 3b we give the corresponding plots for the correlation function  $C_1(t)$  which is obtained by Laplace-inverting (47) numerically.

For short times, there is not much difference between the  $J$ -,  $M$ - and the interpolation model results, as expected. Also when  $\lambda$  is small, the three models agree with each other closely, for all times. However, as  $\lambda$  increases, significant differences start appearing. It is also interesting to note that the  $\gamma=0.5$  plot of  $C_1(t)$  for  $\lambda=2.5$  (cf., figure 3b) lies closer to that of the  $J$ -diffusion model, although in this case, as much

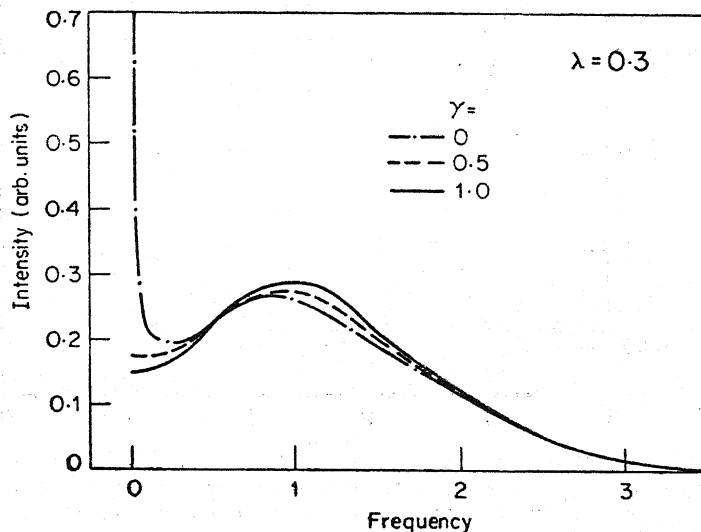


Figure 2a. Infrared line shapes for  $\lambda=0.3$  and  $\gamma=0.0, 0.5$  and  $1.0$ . As mentioned in the text, the frequency is in the reduced units of  $(k_B T/I)^{1/2}$ .

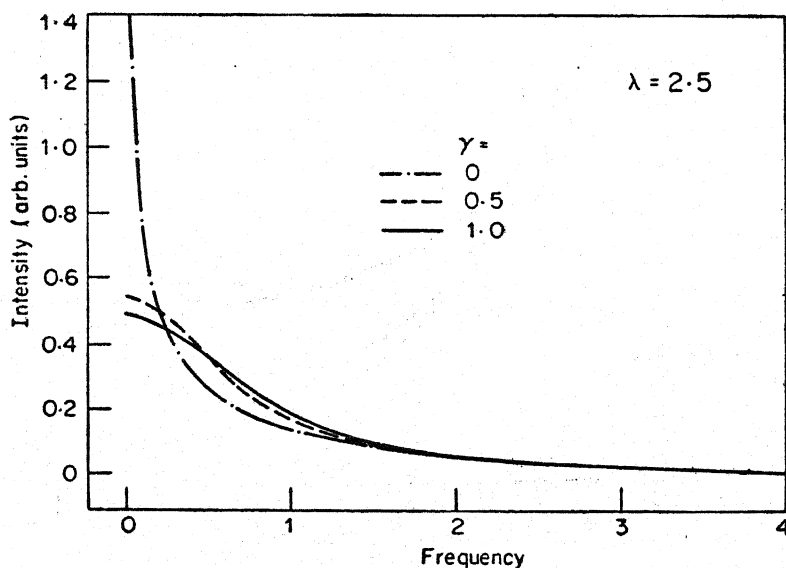


Figure 2b. Infrared line shapes for  $\lambda=2.5$  and  $\gamma=0.0, 0.5$  and  $1.0$ .

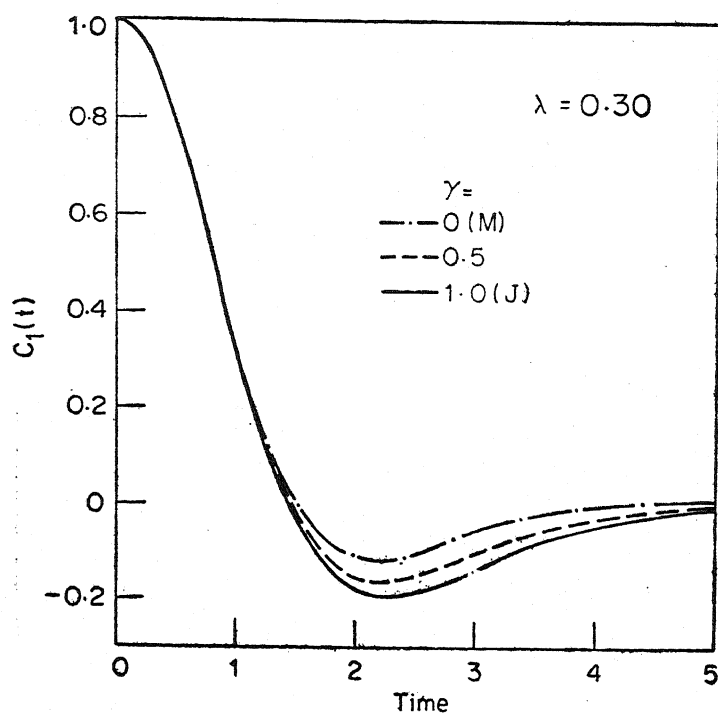


Figure 3a. Dipole correlation functions for  $\lambda=0.3$  and  $\gamma=0.0, 0.5$  and  $1.0$ . These have been obtained by numerical Laplace inversion of spectral profiles plotted in fig. 2(a).

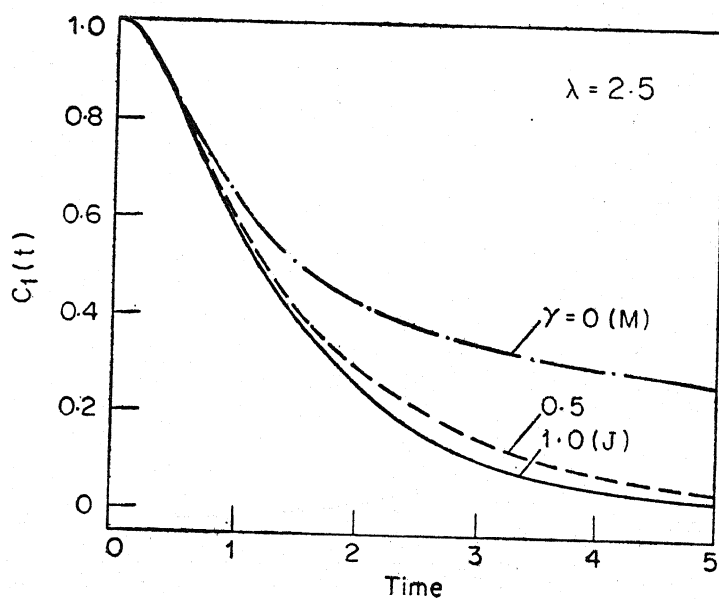


Figure 3b. Dipole correlation functions for  $\lambda=2.5$  and  $\gamma=0.0, 0.5$  and  $1.0$ .

as 50% of the collisions are *M*-like. This is perhaps so in view of the fact that when the rate of collisions is large, an admixture of the *J*-component in the collisions enables the system to be thermalised rapidly.

Apart from the line shape, another interesting quantity to calculate is the rotational correlation time defined as the zeroth moment of the correlation function (Steele 1976):

$$\tau_l = \int_0^{\infty} C_l(t) dt = C_l(p=0), \quad (51)$$

where the second step follows from (28).

Using (47), the correlation time in the interpolation model is given by

$$\tau_l^I = \left[ \left( \int_0^{\infty} d\omega p(\omega) f_1(\lambda) \right)^{-1} - \gamma\lambda \right]^{-1}, \quad (52)$$

where  $p(\omega)$  is given by (27) which, in reduced frequency units, yields

$$p(\omega) d\omega = \omega \exp(-0.5 \omega^2) d\omega. \quad (53)$$

Combining (50), (52) and (53), the correlation time in the infrared case can be easily shown to be

$$\tau_l^I = (\gamma\lambda)^{-1} F(x) [1 - F(x)]^{-1}, \quad (54)$$

$$\text{where } x = \frac{1}{2}\gamma\lambda^2, \quad (55)$$

$$\text{and } F(x) = x \exp(x) E_1(x), \quad (56)$$

$E_1(x)$  being the first exponential integral defined by (cf., Abramowitz and Stegun 1965)

$$E_1(x) = \int_x^{\infty} dt t^{-1} \exp(-t). \quad (57)$$

Therefore, as  $\gamma \rightarrow 0$  (the *M*-diffusion limit),

$$\tau_l^I \rightarrow -\frac{1}{2} \lambda \ln \gamma + \text{finite terms}, \quad (58)$$

which shows precisely how the divergence of  $\tau_l^M$ , an unphysical feature of the *M*-diffusion model as applied to a *linear* molecule, occurs (cf., McClung 1977).

In the limit  $\gamma=1$ , (54) reduces to the expression obtained by Kluc and Powles (1975) in the *J*-diffusion model. We exhibit in figure 4a plot of the correlation time  $\tau_l$  against the collision frequency  $\lambda$  for different values of  $\gamma$  (cf., Steele 1976).

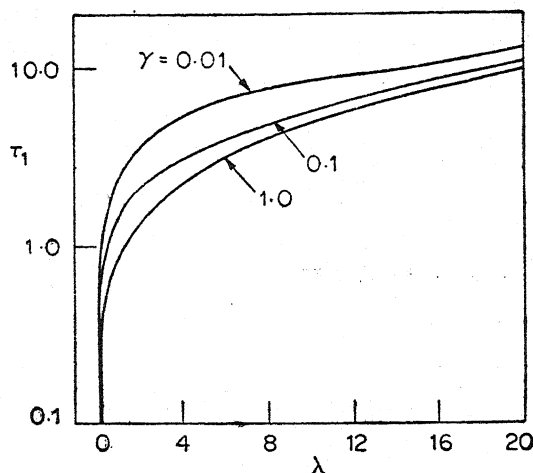


Figure 4. Correlation time  $\tau_1$  for infrared case as a function of the collision frequency  $\lambda$  for  $\gamma=0.01$ ,  $0.1$  and  $1.0$  on semi-logarithmic scales.

#### 4.2. The Raman case

For the Raman line shape,  $l=2$ , and (33) yields

$$\begin{aligned}
 f(p+\lambda) &= \int_0^{\infty} dt \exp [-(p+\lambda)t] d_{00}^{(2)}(\omega t) \\
 &= \left[ (p+\lambda) + \frac{\omega^2}{p+\lambda} \right] [(p+\lambda)^2 + 4\omega^2]^{-1},
 \end{aligned} \tag{59}$$

having used the expression for  $d_{00}^{(2)}(\omega t)$  (Edmonds 1957). The line shape is then deduced from (47) by combining (48) with (59) (see also the appendix B).

The spectral line profiles have been plotted for  $\lambda=1.25$  and  $\lambda=2.5$  in figures 5a and 5b respectively for the same values of  $\gamma$  as have been used in figures 3a and 3b. For Raman line shape, the difference between the  $J$ ,  $M$  and the interpolation models start becoming important for a larger value of  $\lambda$  than that in the infrared case. This is why the smallest value of  $\lambda$  that we consider for Raman plots is  $1.25$  (as opposed to  $0.3$  in the infrared case of figures 2a and 3a). The corresponding correlation functions for the Raman case are shown in figures 6a and 6b. Again, the results for  $\gamma=0.5$  lie closer to those of the  $J$ -diffusion model.

Substituting for  $p(\omega)$  from (53) and  $f_1(\lambda)$  from (48) and (59) into (52), the correlation time in the interpolation model for the Raman case, can be shown to be given by

$$\tau_2^I = (\gamma\lambda)^{-1} \left[ \frac{1}{3} (3+\gamma) (1-F(x))^{-1} - 1 \right], \tag{60}$$

$$\text{where } x = \gamma\lambda^2 (6 + 2\gamma)^{-1}, \tag{61}$$

and  $F(x)$  is defined by (56).

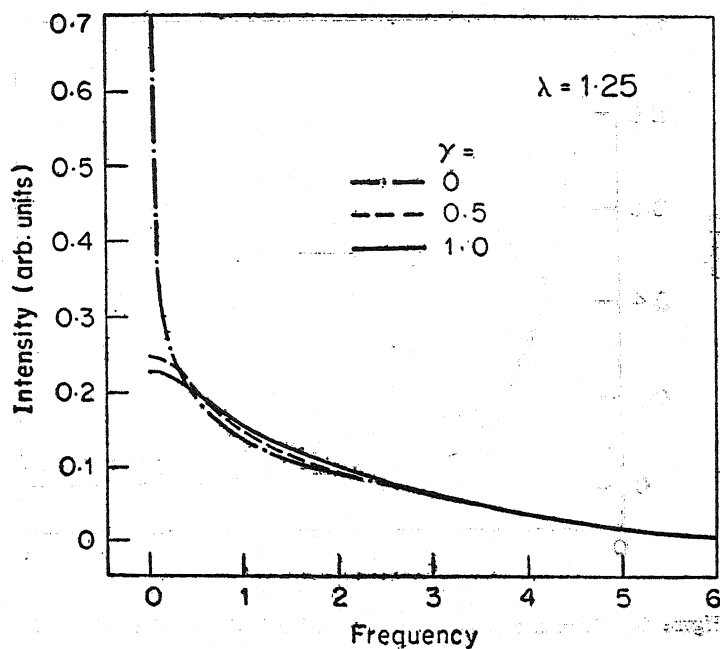


Figure 5a. Raman lineshapes for  $\lambda=1.25$  and  $\gamma=0.0, 0.5$  and  $1.0$ .

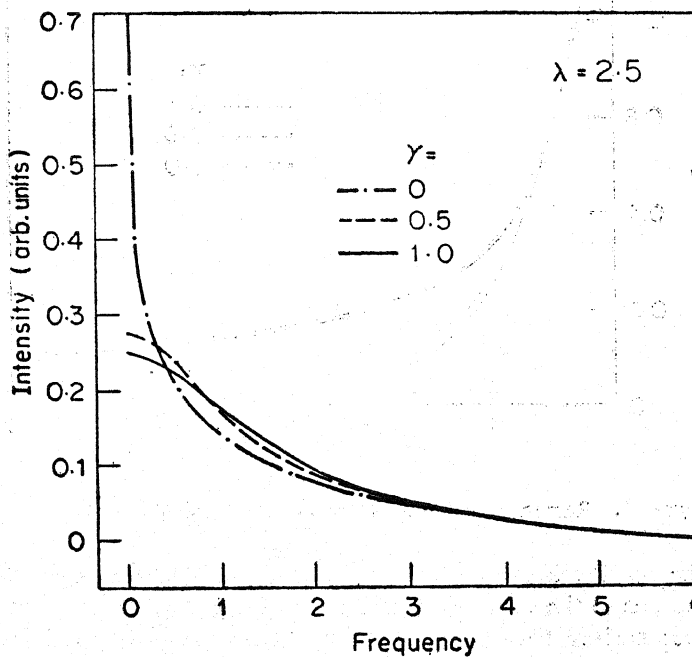


Figure 5b. Raman lineshapes for  $\lambda=2.5$  and  $\gamma=0.0, 0.5$  and  $1.0$ .

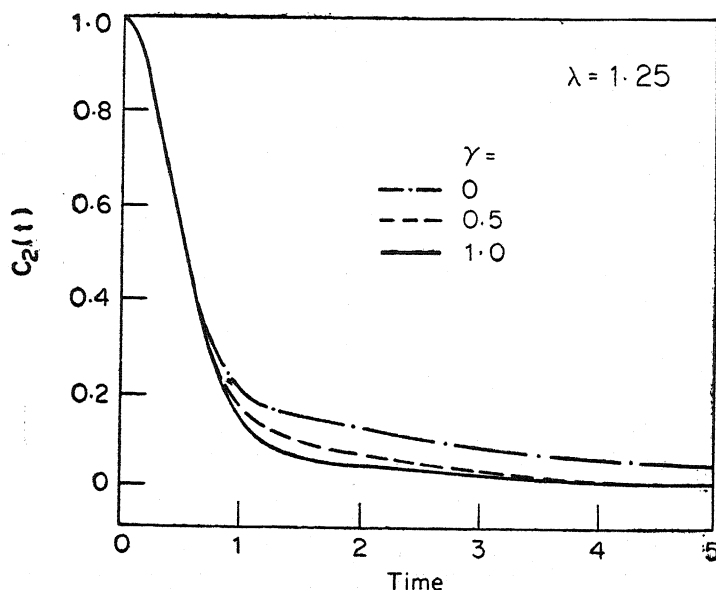


Figure 6a. Raman correlation functions for  $\lambda=1.25$  and  $\gamma=0.0, 0.5$  and  $1.0$ .

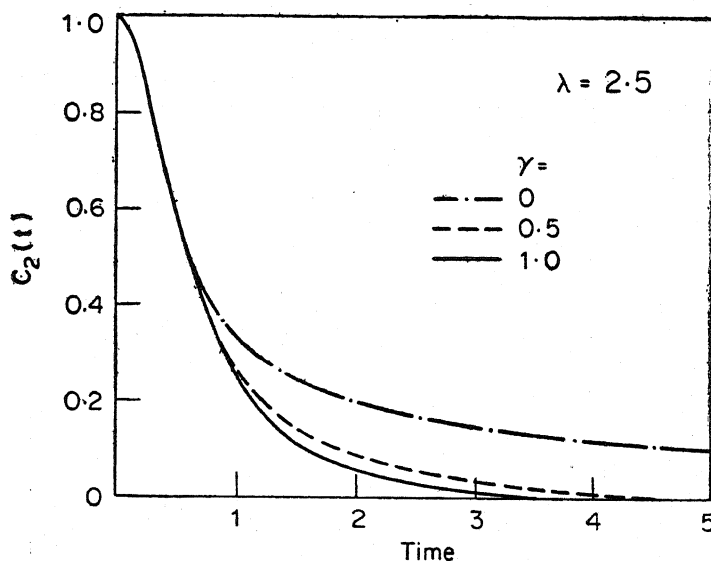


Figure 6b. Raman correlation functions for  $\lambda=2.5$  and  $\gamma=0.0, 0.5$  and  $1.0$ .

Again, in the  $M$ -diffusion model ( $\gamma=0$ ),  $\tau_2^-$  diverges while in the  $J$ -diffusion limit ( $\gamma=1$ ), (60) reduces to the expression derived by Kluc and Powles (1975). In order to make the comparison between our results and those of Kluc and Powles transparent, we plot in figure 7, the correlation time versus the inverse of collision frequency on a log-log scale for various values of  $\gamma$ .



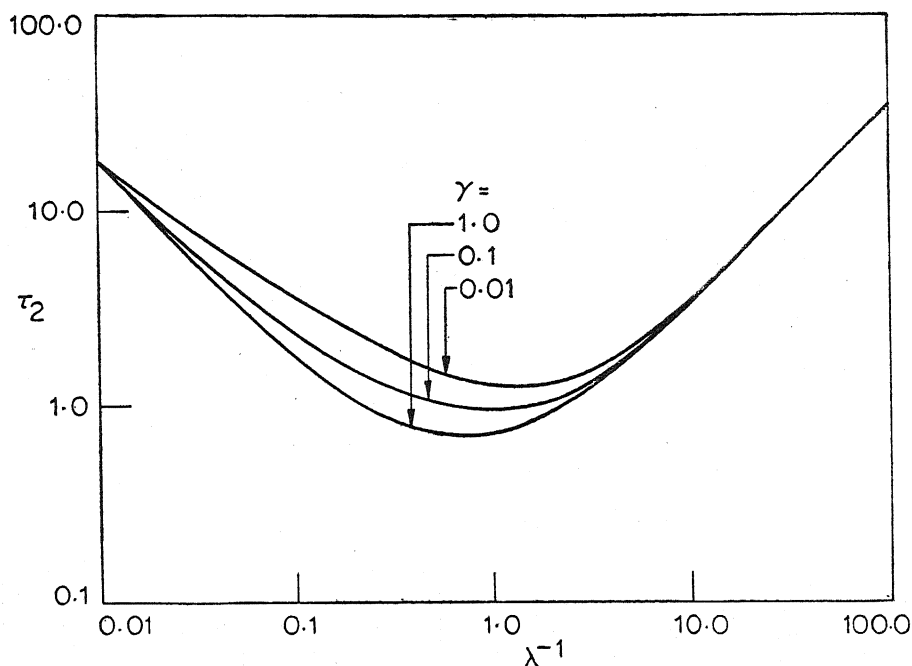


Figure 7. Correlation time  $\tau_2$  for Raman case as a function of the inverse of the collision frequency for  $\gamma=0.01$ ,  $0.1$  and  $1.0$  on logarithmic scales.

## 5. Comparison with experiments

As stated in §1, experimental data on molecular relaxation studies fall in many cases between the two extreme limits of the  $J$ - and  $M$ -diffusion models. In such situations, the interpolation model can give a better interpretation of the data. We discuss this below by comparing our results with a couple of examples from infrared experiments on CO dissolved in  $N_2$  and nuclear relaxation studies on HBr.

### 5.1. Infrared studies on CO dissolved in $N_2$

Marsault *et al* (1975) have carried out extensive infrared measurements on the linear molecular system of carbon monoxide in various host fluids. The rotational motion is investigated by studying the fundamental vibrational band of CO over a wide range of temperatures and pressures.

We discuss here the data obtained for CO dissolved in  $N_2$  at a fixed pressure of 80 bar and at various temperatures. At 158°K, the host  $N_2$  is in a dense gas form and the experimental rotational correlation function is well described by the  $M$ -diffusion model. On the other hand, at 116°K,  $N_2$  is in the form of a dense liquid and the data are fitted well by the  $J$ -diffusion model. However, at intermediate temperatures such as 129°K, neither the  $M$ - nor the  $J$ -diffusion model gives a satisfactory account of the data (figure 8). As can be clearly seen from the figure, values of  $\lambda=0.5$  and  $\gamma=0.3$  in the interpolation model fit the experimental points at 129°K very well. The fit to the data at other temperatures requires a change in the values of both  $\lambda$  and  $\gamma$ .

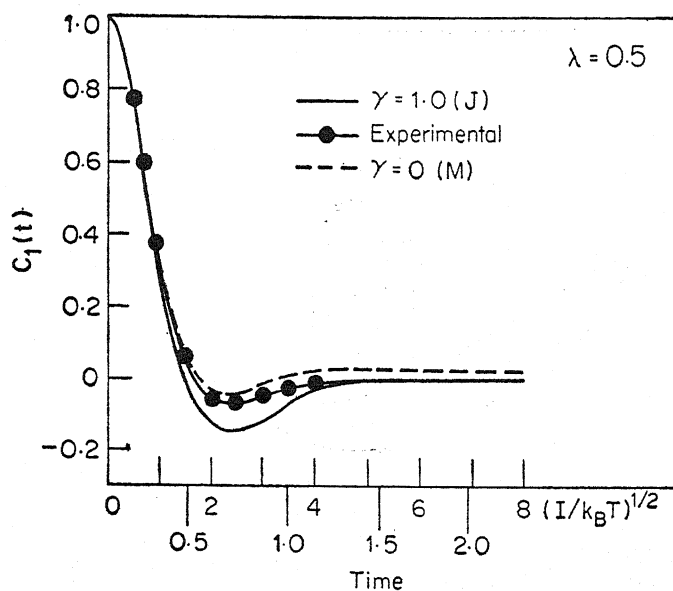


Figure 8. Dipole correlation function for CO dissolved in nitrogen. The dashed line is the experimental curve from Marsault *et al* (1975) corresponding to  $P=80$  bar and  $T=129^\circ\text{K}$ .  $\bullet$  are the points calculated from our theory for  $\gamma=0.30$ . The correlation functions for  $\gamma=0.0$  ( $M$ -diffusion) and  $\gamma=1.0$  ( $J$ -diffusion) have also been shown for comparison.

### 5.2. Nuclear spin-relaxation studies on HBr

An independent experimental tool to study molecular rotational motion is the measurement of nuclear spin-lattice relaxation (Gordon 1966). The latter can yield a determination of the parameter  $\lambda$ , the collision frequency that appears in the models described here. The applicability of these models may therefore be directly tested by comparing nuclear relaxation data with infrared and Raman band shapes.

Based on the experimental results of Krynicki and Powles (1972) on nuclear spin-relaxation in the linear molecular system of HBr, Kluc and Powles (1975) have deduced a plot of the Raman correlation time  $\tau_2$  versus the inverse of collision frequency (in reduced units) on a logarithmic scale. It is seen that the  $J$ -diffusion model does not lead to an agreement with the data points (figure 9). We find that values of  $\gamma$  lying in the range 0.05 to 0.1 explain the experimental data satisfactorily.

## 6. Conclusions

In this paper, we have presented an attempt to generalise the extended diffusion models of Gordon with a view to applying the theory to molecular rotation data of systems whose behaviour is intermediate between those pictured by the  $M$ - and  $J$ -limits. The mathematical formulation of our theory retains the simple basic idea of Gordon in which intermolecular torques are assumed to be random. The latter aspect is modelled in terms of abrupt collisions which are assumed to interrupt the free rotations of the molecule. The introduction of a collision operator  $\mathcal{T}$  in the theory, which enables us to generalise the EDM, is made possible by following parallel theoretical develop-

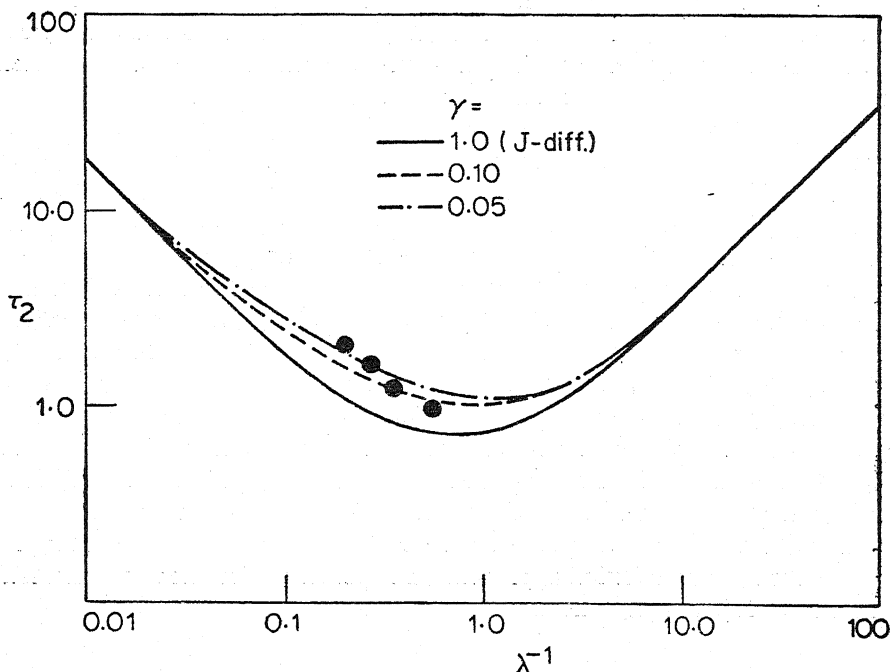


Figure 9. Plot of correlation time  $\tau_2$  versus inverse of collision frequency on logarithmic scales. The experimental results for HBr as deduced by Kluc and Powles (1975) are shown as O. The solid lines are the theoretical curves from our theory for  $\gamma=0.05$  0.10 and 1.0.

ments in other line shape analyses (see § 2.3). In particular, we might mention that the assumption involved in the *J*-diffusion model (cf., equation (34)) is referred to as a kind of random phase approximation in the theory of line shapes (Dattagupta 1977a); it is also sometimes known as the strong collision approximation in the collision broadening theory (Dattagupta 1977b).

It is evident from the discussions in § 3 that the *J*-diffusion model (or, equivalently, the strong collision model) applies to the case in which there is no persistence or 'hang-over' in a collision as far as the angular speed is concerned. In contrast, in the *M*-diffusion model, there is complete persistence of angular speed at every collision (cf., (31)). In the collision broadening theory, it is a common practice to treat the opposite of the strong collision limit, called the weak collision model, in which it is assumed that there is significant persistence of the angular speed in every collision step. The collision operator  $\mathcal{T}$ , in the weak collision limit, is assumed to satisfy a Fokker-Planck like equation (for instance, see Dattagupta 1977c). The weak collision model, when applied to the present problem, resembles closely the Langevin model of Fixman and Rider (1969). There also exist in the literature schemes for describing situations intermediate between the weak and strong collision limits (Keilson and Storer 1952; Rautian and Sobel'man 1967). Attempts to incorporate these schemes into the collision operator  $\mathcal{T}$  for determining the correlation function  $C_i(t)$  are much more complicated than the simple interpolation model described here (§ 3.3) but should be interesting to investigate.

Notwithstanding their success in explaining data in the dense phase, both the EDM as well as the generalised model presented here, suffer from the fact that they are based on a picture of instantaneous collisions. These models therefore ignore the memory effects which can be very important in dense liquids, especially near the freezing point (Marsault *et al* 1975). The most general approach to handle such memory effects is the one due to Mori (1965 a, b) which has been adapted into the present field by Berne and Harp (1970) and Bliot *et al* (1972). However, the practical applications of the memory function formalism almost always involve construction of memory kernels on a rather ad-hoc fashion (see, for example, Berne and Harp 1970, Marsault *et al* 1975). There do not appear to be systematic derivations of the memory kernels in a specific physical situation apart from some procedure of checking their validity by comparison with moment calculations. It may be pointed out that the free rotational motion incorporated in the EDM by Gordon constituted what amounts to inertial memory effects that were absent in the earlier models which were based on Debye's idea of rotational diffusion (Hubbard 1963). It would be interesting to extend the simple physical idea of the Gordon-type models (as discussed in this paper) to cover situations in which 'other' memory effects arising from intermolecular potentials become important. This will enable us to establish a connection between the present study and the memory function approach. Such attempts are underway now and the results will be reported elsewhere.

### Acknowledgements

The authors are grateful to G Venkataraman for his continual encouragement throughout the course of this work. They should thank also A P Roy for valuable discussions and B Purniah for help in computations. SD acknowledges an illuminating conversation with V Balakrishnan on the material presented in appendix A. Finally the authors thank one of the referees for pointing out the connection between the interpolation model treated here and the relaxation model considered by Fixman and Rider.

### Appendix A

#### *Meaning of the interpolation parameter $\gamma$*

Three distinct features are noteworthy in the interpolation model discussed in this paper and the EDM of Gordon. They are (i) free rotation, (ii) randomisation of the direction of the angular velocity and (iii) randomisation of the magnitude of the angular velocity. The last two points are simply a statement of the fact that the random variable in the present problem is a vector. Let us now inquire into the time-scales that are associated with the three aspects of the motion mentioned above. The time which sets the scale of free rotation is obviously  $(I/k_B T)^{1/2}$ . Next, the time-scale on which randomisation of the direction of angular velocity occurs, is the same as the mean-free time between collisions, both in the EDM and in the interpolation model. However, the time-scale on which randomisation of the angular

speed takes place, is different in the  $M$ ,  $J$  and the interpolation models. It is this last aspect of the problem that we wish to discuss in the following.

Let us restrict our attention to only that part of the stochastic space which contains the one-dimensional variable  $\omega$ , the angular speed, and examine the structure of  $(\omega | P(t) | \omega_0)$  which defines the conditional probability that in time  $t$ , the stochastic variable assumes the value  $\omega$ , given that it was  $\omega_0$  at  $t=0$ . In terms of the model described in § 2.2, the  $P$ -matrix can be shown to be given by (Dattagupta 1977c)

$$P(t) = \exp [\lambda (\mathcal{T} - 1) t], \quad (\text{A1})$$

Equation (A1) is the solution of the Chapman-Kolmogorov-Smoluchowski equation which describes a stationary Markov process (see for instance Van Kampen 1976).

Now, in the interpolation model (cf., (43)),

$$\mathcal{T} = \mathcal{T}_1 + (1-\gamma) (1-\mathcal{T}_1), \quad (\text{A2})$$

where  $\mathcal{T}_1$  is defined by (44). It is easy to see that

$$\begin{aligned} (\omega | \mathcal{T}_1^2 | \omega_0) &= \int d\omega' (\omega | \mathcal{T}_1 | \omega') (\omega' | \mathcal{T}_1 | \omega_0) \\ &= (\omega | \mathcal{T}_1 | \omega_0), \quad \text{from (44).} \end{aligned}$$

This implies that  $\mathcal{T}_1$  is the idempotent matrix which satisfies the relations

$$\begin{aligned} \mathcal{T}_1^n &= \mathcal{T}_1 \quad (n \geq 1), \\ \mathcal{T}_1 (1-\mathcal{T}_1) &= 0 \\ (1-\mathcal{T}_1)^2 &= 1-\mathcal{T}_1, \text{ etc.} \end{aligned} \quad (\text{A3})$$

Using (A2) and (A3) in (A1), it is straightforward to show by direct power series expansion that

$$P(t) = \mathcal{T}_1 + (1-\mathcal{T}_1) \exp (-\gamma \lambda t). \quad (\text{A4})$$

Therefore, in the  $J$ -diffusion limit ( $\gamma = 1$ ),

$$(\omega | P(t) | \omega_0) = p(\omega) + [\delta(\omega - \omega_0) - p(\omega)] \exp (-\lambda t), \quad (\text{A5})$$

while in the  $M$ -diffusion limit ( $\gamma = 0$ ),

$$(\omega | P(t) | \omega_0) = \delta(\omega - \omega_0). \quad (\text{A6})$$

Equations (A5) and (A6) imply that the time scale on which the angular speed is randomised is  $\lambda^{-1}$  in the  $J$ -diffusion model while it is  $\infty$  in the  $M$ -diffusion case. On the other hand, the corresponding time-scale is  $(\gamma \lambda)^{-1}$  in the interpolation model (cf., (A4)). Thus  $(\gamma \lambda)$  is an *effective* rate at which collisions change the angular speed.

It is clear that the origin of  $\gamma$  lies in the strength of the interaction that the 'molecule of interest' feels when it is hit by a perturber. It is also clear that in many liquids, the  $J$ -diffusion model overestimates the average effectiveness of a collision as far as the randomisation of the angular speed is concerned. The interpolation model cures this disease, in the simplest possible way, by scaling down the relaxation rate from  $\lambda$  to  $(\gamma\lambda)$ .

We refer the reader to the work of Balakrishnan (1979) for further discussions on the time-scaling properties of the interpolation model.

## Appendix B

We give below the expressions which have been used in Section 4 for computation of infrared and Raman line shapes.

The line shape in the infrared case is given by

$$I_{IR}(s) = (\pi)^{-1} [Z_1(1-\gamma\lambda Z_1) - \gamma\lambda Z_2^2] [(1-\gamma\lambda Z_1)^2 + \gamma^2\lambda^2 Z_2^2]^{-1}, \quad (B1)$$

where

$$Z_1(s) = \int d\omega p(\omega) A(s, \omega)/B(s, \omega),$$

$$Z_2(s) = \int d\omega p(\omega) C(s, \omega)/B(s, \omega),$$

$$A(s, \omega) = \lambda(\omega^2 - s^2 + \gamma\lambda^2) + \omega^2(\lambda + \gamma\lambda), \quad (B2)$$

$$B(s, \omega) = (\omega^2 - s^2 + \gamma\lambda^2)^2 + s^2(\lambda + \gamma\lambda)^2,$$

$$C(s, \omega) = \lambda s(\lambda + \gamma\lambda) - s(\omega^2 - s^2 + \gamma\lambda^2).$$

The Raman line shape is given by

$$I_R(s) = (\pi)^{-1} [Z_3(1-\gamma\lambda Z_3) - \gamma\lambda Z_4^2] [(1-\gamma\lambda Z_3)^2 + \gamma^2\lambda^2 Z_4^2]^{-1}, \quad (B3)$$

where

$$Z_3(s) = \int d\omega p(\omega) [E(1-\beta E) - \beta F^2] [(1-\beta E)^2 + \beta^2 F^2]^{-1}$$

$$Z_4(s) = \int d\omega p(\omega) [F(1-\beta E) + \beta EF] [(1-\beta E)^2 + \beta^2 F^2]^{-1},$$

$$\beta = \lambda(1-\gamma),$$

$$E = 0.25\lambda G + 0.75\lambda(2s^2 + H)R, \quad (B4)$$

$$F = 0.25sG + 0.75s(2\lambda^2 - H)R,$$

$$G = (\lambda^2 + s^2)^{-1},$$

$$H = (\lambda^2 + 4\omega^2 - s^2),$$

$$R = (H^2 + 4\lambda^2 s^2)^{-1}.$$

## References

- Abramowitz and Stegun I A 1965 *Handbook of mathematical functions* (New York: Dover)
- Balakrishnan V 1979 *Pramana* **13**
- Berne B J and Harp G D 1970 *Adv. Chem. Phys.* **17** 63
- Berne B J and Pecora R 1976 *Dynamic light scattering* (New York: John Wiley)
- Bliot F, Abbar C and Constant E 1972 *Mol. Phys.* **24** 241
- Clauser M J and Blume M 1971 *Phys. Rev.* **B3** 583
- Dattagupta S 1975 *Phys. Rev.* **B12** 47
- Dattagupta S 1977a *Phys. Rev.* **B16** 158
- Dattagupta S 1977b *Pramana* **9** 203
- Dattagupta S 1977c *Nucl. Phys. Solid State Phys. (India)* **A20** 19
- Edmonds A R 1957 *Angular momentum in quantum mechanics* (Princeton: University Press)
- Favro L D 1960 *Phys. Rev.* **53** 119
- Fixman M and Rider K 1969 *J. Chem. Phys.* **51** 2425
- Gordon R G 1966 *J. Chem. Phys.* **44** 1830
- Gordon R G 1968 *Adv. Magn. Reson.* **3** 1
- Hubbard P S 1963 *Phys. Rev.* **131** 1155
- Keilson J and Storer J E 1952 *Q. J. Appl. Maths.* **10** 243
- Kluc E and Powles J G 1975 *Mol. Phys.* **30** 1109
- Krynicky K and Powles J G 1972 *J. Magn. Reson.* **6** 539
- Marsault J P, Marsault-Herail F and Levi G 1975 *J. Chem. Phys.* **62** 893
- McClung R E D 1969 *J. Chem. Phys.* **51** 3842
- McClung R E D 1971a *J. Chem. Phys.* **54** 3248
- McClung R E D 1971b *J. Chem. Phys.* **55** 3459
- McClung R E D 1972 *J. Chem. Phys.* **57** 5478
- McClung R E D 1977 *Adv. Mol. Relaxation Processes* **10** 88
- Mori H 1965a *Prog. Theor. Phys.* **33** 423
- Mori H 1965b *Prog. Theor. Phys.* **34** 399
- Mountain R D 1971 *J. Chem. Phys.* **54** 3243
- Rautian S G and Sobel'man I I 1967 *Sov. Phys. Usp.* **9** 701
- Steele W A 1976 *Adv. Chem. Phys.* **34** 1
- St. Pierre A G and Steele W A 1972 *J. Chem. Phys.* **57** 4638
- Van Kampen N G 1976 *Phys. Rep.* **24** 171